Arbutamine Stress Perfusion Imaging in Dogs with Critical Coronary Artery Stenoses: ^{99m}Tc-Sestamibi Versus ^{201}Tl

Mirta Ruiz, MD; Kazuya Takehana, MD; Frank D. Petruzella, BA; Denny D. Watson, PhD; George A. Beller, MD; and David K. Glover, ME

Experimental Cardiology Laboratory, Cardiovascular Division, Department of Medicine, University of Virginia Health System, Charlottesville, Virginia

Having previously shown that dobutamine reduces ^{99m}Tc-methoxyisobutylisonitrile (sestamibi [MIBI]) uptake in normal myocardium by elevating intracellular calcium, we hypothesized that arbutamine, which has less inotropic effect than dobutamine, might cause less reduction in MIBI uptake, thereby improving defect contrast. In this study using a canine model, we compared the effects of arbutamine stress on myocardial blood flow, myocardial MIBI uptake, and systolic thickening in the presence of a coronary artery stenosis. **Methods:** Arbutamine was infused (0.5–250 ng/kg/min) in 8 open-chest dogs with critical coronary stenoses that abolished flow reserve. At the time of peak arbutamine effect, MIBI (296 MBq), ^{201}Tl (27.75 MBq), and microspheres were coinjected. The dogs were killed 5 min later, and myocardial tracer activities and flow were quantified by well counting. Ex vivo imaging of heart slices was also performed. **Results:** Arbutamine increased mean heart rate, peak positive left ventricular pressure and its first time-derivative, and normal-zone myocardial thickening. Stenotic zone flow and thickening did not increase during arbutamine infusion. MIBI uptake versus flow was significantly lower than ^{201}Tl uptake at the same flow values. By imaging, defect magnitude (stenotic/normal) was greater for ^{201}Tl than MIBI (0.56 vs. 0.57; $P < 0.001$). **Conclusion:** In the presence of coronary stenoses that abolished regional flow reserve, myocardial uptake of MIBI, compared with ^{201}Tl, significantly underestimated the arbutamine-induced flow heterogeneity. The attenuation of MIBI uptake and diminished defect contrast during arbutamine stress were comparable with those previously reported for dobutamine stress.

Key Words: arbutamine; ^{99m}Tc-sestamibi; coronary disease

J Nucl Med 2002; 43:664–670

Exercise myocardial perfusion imaging is a well-known technique for evaluation of coronary artery disease, but an estimated 30%–50% of patients requiring cardiac stress testing cannot exercise adequately (*1*). These patients require pharmacologic stress imaging with either a vasodilator or an inotropic agent.

Our previous studies have shown that uptake of ^{99m}Tc-methoxyisobutylisonitrile (sestamibi [MIBI]) is attenuated during dobutamine stress, when compared with ^{201}Tl uptake administered simultaneously (*2*). Also, MIBI defects produced by dobutamine are less pronounced than adenosine-induced defects at the same flow heterogeneity between normal and stenotic zones (*1–15*). The reduction in defect magnitude has been attributed to altered mitochondrial membrane binding of MIBI consequent to the enhanced Ca^{2+} flux produced by dobutamine. MIBI uptake can be enhanced during dobutamine infusion with the injection of ruthenium red, a selective inhibitor of mitochondrial calcium influx (*2,5,16,17*). Arbutamine (1,2-benzenodiol,4-[1-hydroxy-2[[4(-hydroxyphenyl)butyl]amino]ethyl]hydrochloride (*1,10–14*)) is a short-acting synthetic potent nonselective β-adrenoceptor agonist that increases heart rate, cardiac contractility, and systolic blood pressure. Arbutamine has mild α_1-sympathomimetic activity. This agent was developed as a cardiac pharmacologic stressor to be used in conjunction with echocardiography or radionuclide perfusion imaging (*10, 13,18*).

We sought to determine whether the more mild inotropic effect of arbutamine infusion, compared with dobutamine, might result in less attenuation of myocardial MIBI uptake. If this hypothesis were correct, arbutamine-induced MIBI defects would better reflect stenosis severity and abnormal flow reserve.

MATERIALS AND METHODS

Surgical Preparation

Eight fasting adult mongrel dogs (mean weight, 26.91 kg) were anesthetized with intravenous sodium pentobarbital (30 mg/kg), tracheally intubated, and mechanically ventilated with room air (Harvard Apparatus, Inc., Holliston, MA) with a positive end-expiratory pressure of 4 cm water. Arterial blood gases were monitored (model 158; Ciba-Corning Diagnostics Corp., Medfield, MA) and maintained in the normal physiologic range. The left femoral vein was cannulated with an 8-French catheter for the

Received Sep. 10, 2001; revision accepted Jan. 22, 2002.

For correspondence or reprints contact: Mirta Ruiz, MD, Cardiovascular Division, Department of Medicine, University of Virginia Health System, P.O. Box 800500, Charlottesville, VA 22908-0500.

E-mail: mrh2v@virginia.edu

administration of fluids, MIBI, ^{201}Tl, and sodium pentobarbital. Both femoral arteries were cannulated with 8-French catheters and used for radiolabeled microsphere reference blood withdrawal. A 7-French high-fidelity pressure catheter (Millar Instruments, Inc., Houston, TX) was inserted into the left ventricle through an 8-French sheath in the left carotid artery for arterial pressure monitoring. The left external jugular vein was cannulated with an 8-French catheter for administration of arbutamine.

A left lateral thoracotomy was performed at the level of the fifth intercostal space, and the heart was suspended in a pericardial cradle. A catheter was inserted into the left atrium for pressure measurement and for the injection of microspheres. A snare ligature was loosely placed on a proximal portion of the left anterior descending coronary artery (LAD). Ultrasonic flow probes (T201; Transonic Systems Inc., Ithaca, NY) were placed on a more distal portion of the LAD and on the left circumflex coronary artery (LCX). Regional systolic thickening was measured by pulsed-Doppler technique using epicardial sonomicrometer crystals (Crystal Biotech Inc., Northborough, MA), which were sutured to the epicardium in regions supplied by the LAD and LCX for measurement of regional systolic thickening. Throughout the protocol, the electrocardiogram, arterial and left atrial pressures, LAD and LCX flows, myocardial thickening, and left ventricular pressure and its first time-derivative (dP/dt) were continuously recorded on a 16-channel thermal-array-strip chart recorder (K2G; Astro-Med, Inc., West Warwick, RI) and simultaneously digitized and stored in real time onto an IBM-compatible personal computer equipped with a 750-MHz Pentium processor (Intel Corp., Santa Clara, CA) and an optical drive.

All experiments were performed with the approval of our institution's Animal Research Committee and were in compliance with the position of the American Heart Association on the use of research animals.

Experimental Protocol

Thirty minutes after instrumentation, baseline microspheres were injected to determine myocardial blood flow (Fig. 1). To measure the normal reactive hyperemic response, the LAD was occluded for 10 s, and the peak flow that followed was recorded on the strip chart. The snare ligature was then adjusted to create an LAD stenosis that abolished the normal reactive hyperemic response without reducing resting flow (*16*). Microspheres were injected 15 min later to determine myocardial flow in the presence of the stenosis. Arbutamine was then infused intravenously in 7-min dose increments of 5, 10, 50, 100, and 250 ng/kg/min (model 3400 infusion pump; Graseby Medical Ltd., Herts, U.K.). Microspheres were injected simultaneously with MIBI (296 MBq) and ^{201}Tl (27.75 MBq) at the arbutamine peak dose of 250 ng/kg/min. The dogs were killed 5 min later by an overdose of sodium pentobarbital.

Determination of Regional Myocardial Systolic Thickening

Regional systolic thickening was measured by the epicardial crystal pulsed-Doppler technique (*2*,*3*). This technique is atraumatic, has been previously validated in the canine model, and has been used extensively by our group. The depth of the endocardial–left ventricular cavity interface during maximal diastolic thinning was determined by oscilloscope display of the Doppler signal, and the pulsed-Doppler sample volume was placed at this depth. Myocardial systolic thickening was measured as the net increase in wall thickness from the onset to the end of systole, as defined by the initial upward and peak negative deflections of the left ventricular dP/dt tracings, respectively. Relative systolic thickening (thickening fraction) was calculated as follows: ((end-systolic thickness − end-diastolic thickness) ÷ end-diastolic thickness) × 100%. Thickening was measured over at least 1 respiratory cycle during the last minute of each stage of the protocol, and the highest measured values were reported (excluding beats that occurred after ventricular ectopy).

Ex Vivo Slice Imaging

After the dogs were killed, the hearts were removed and sliced into 4 rings approximately 1 cm thick from apex to base. The slices were trimmed of excess fat and adventitia and placed on a piece of cardboard covered with cellophane wrap. The slices were imaged directly on the collimator, with a standard gamma camera and computer (model 420; Ohio-Nuclear/Technicare, Solon, Ohio) using an all-purpose, low- to medium-energy collimator with a 20% window centered on the MIBI photopeak, and the images were recorded using a 128 × 128 matrix for a total of 10^6 counts. Twenty-four hours later, the slices were reimaged using a 25% window centered on the ^{201}Tl photopeak, with the same matrix, for a total of 1,638 s. Only the 2 center slices were quantified, because the basal slice was above the stenosis and the apical slice lacked a quantifiable normal area. A region of interest (ROI) was drawn on the anteroapical wall to represent the stenotic zone, and a second ROI was drawn on the normal posterior wall. The stenotic-to-normal count ratio was calculated by dividing the counts per pixel in the stenotic ROI by the counts per pixel in the normal ROI. The stenotic-zone ROI was drawn to include the MIBI perfusion defect (if visible) and was limited to an area of the left ventricle in the central stenotic zone. The normal-zone ROI was limited to the left ventricle in the area with maximal myocardial counts.

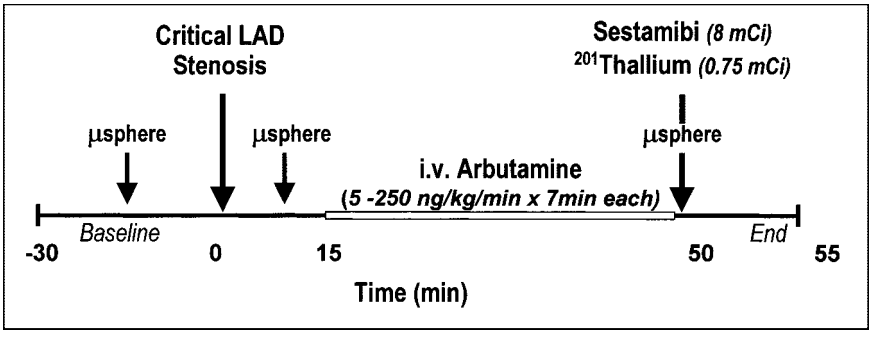

FIGURE 1. Experimental protocols. μsphere = microspheres.

TABLE 1
Hemodynamic Parameters

Parameter	Baseline	Stenosis	Arbutamine (ng/kg/min) 5	10	50	100	250
Heart rate (bpm)	124 ± 5	123 ± 5	133 ± 5*	141 ± 5*	176 ± 7*	192 ± 7*	208 ± 9*
MAP (mm Hg)	113 ± 5	114 ± 6	112 ± 6	111 ± 6	102 ± 6	98 ± 7	86 ± 7†
LAP (mm Hg)	6.3 ± 0.4	7.1 ± 0.4	6.1 ± 0.3	6.0 ± 0.33	6.4 ± 0.5	6.4 ± 0.5	6.8 ± 0.6
dP/dt (mm Hg/s)	2,188 ± 141	2,201 ± 111	2,489 ± 199	2,921 ± 277†	4,063 ± 258*	4,452 ± 238*	4,372 ± 453*
LAD flow (mL/min)	23 ± 3	18 ± 2	19 ± 2†	20 ± 2	20 ± 2†	21 ± 2	17 ± 2
LCX flow (mL/min)	31 ± 4	31 ± 5	36 ± 6*	41 ± 7*	58 ± 9*	60 ± 9*	68 ± 11*

*$P < 0.001$ vs. stenosis.
†$P < 0.05$ vs. stenosis.
MAP = mean arterial pressure; LAP = left atrial pressure.
Values are expressed as mean ± SEM.

Determination of Regional Myocardial Blood Flow and MIBI Activity

The microsphere technique used in our laboratory has been described previously (*4*). To measure regional MIBI activity and microsphere-determined blood flow, each of 4 left ventricular slices was divided into 6 transmural sections, which were then subdivided into epicardial, midmural, and endocardial segments. The resulting 72 myocardial tissue samples were counted in a γ-well scintillation counter (MINAXI 5550; Packard Instrument Co., Inc., Downers Grove, IL) for MIBI at 24 h of collection, for ^{201}Tl 72 h later, and for flow 3 wk after ^{201}Tl decay. The window settings on the γ-counter were 50–100 keV for ^{201}Tl, 120–160 keV for ^{99m}Tc, 340–440 keV for ^{113}Sn, 450–580 keV for ^{85}Sr, 680–840 keV for ^{95}Nb, and 842–1,300 keV for ^{46}Sc. The tissue counts were corrected for background, decay, and isotope spillover, and regional myocardial blood flow was calculated with computer software (PCGERDA; Scientific Computing Solutions Inc., Charlottesville, VA). Flow, MIBI activity, and ^{201}Tl activity for each of the 24 transmural sections were calculated as the weighted average of the 3 corresponding epicardial, midmural, and endocardial segments. The stenotic region was defined as the 3 transmural sections with the lowest flows at the time of MIBI and ^{201}Tl injection, and the normal region was defined as the 3 transmural sections with the highest flows. Stenotic-to-normal ratios for flow, MIBI activity, and ^{201}Tl activity were calculated by dividing the average flow, MIBI activity, and ^{201}Tl activity in the stenotic region by the average values in the normal region.

Statistical Analysis

All statistical computations were made with SYSTAT software (SPSS Inc., Chicago, IL). The results are expressed as mean ± SEM. Differences between means within a group were assessed by a repeated-measures ANOVA or by a paired *t* test with $P < 0.05$ considered significant. Comparisons between groups were made with 1-way ANOVA and Tukey post hoc testing.

RESULTS

Hemodynamics

The hemodynamic parameters were not affected by placement of the LAD stenoses (Table 1). The peak dose of arbutamine was achieved in all dogs, and no sustained ventricular or supraventricular arrhythmias occurred during infusion. The mean heart rate was 123 ± 5 bpm during stenosis and increased to 208 ± 9 bpm at the time of peak arbutamine, and peak positive left ventricular dP/dt increased from 2,201 ± 111 to 4,372 ± 453 mm Hg/s ($P < 0.001$ vs. stenosis). The dP/dt increased during arbutamine stress, as was expected. Mean ultrasonic flow in the normal LCX artery increased significantly during arbutamine infusion, from 31 ± 5 to 68 ± 11 mL/min ($P < 0.001$ vs. stenosis). In the stenotic LAD artery, flow reserve was not observed (18 ± 2 to 17 ± 2 mL/min, $P < 0.05$).

Regional Myocardial Systolic Thickening

Regional myocardial systolic thickening was unchanged by placement of the LAD stenoses (Table 2). In the normal zone, relative systolic thickening increased significantly during arbutamine infusion. In the stenotic zone, a flat response to arbutamine infusion was seen, with a failure to

TABLE 2
Systolic Wall Thickening

Relative thickening (%)	Baseline	Stenosis	Arbutamine (ng/kg/min) 5	10	50	100	250
Stenotic	22.7 ± 2.8	21.2 ± 2.4	24.6 ± 2.4*	21.6 ± 2.6	21.5 ± 2.4	21.0 ± 2.4	16.4 ± 3.7
Normal	17.9 ± 2.2	16.3 ± 1.8	17.7 ± 2.6	17.6 ± 1.6	21.7 ± 2.2	22.7 ± 2.4	23.0 ± 2.7

*$P < 0.05$ vs. stenosis.
Relative thickening = [(systolic thickness − diastolic thickness)/diastolic thickness] × 100%. Values are expressed as mean ± SEM.

TABLE 3
Absolute Regional Myocardial Blood Flow

Region	Stenotic zone			Normal zone		
	Baseline	Stenosis	Peak arbutamine	Baseline	Stenosis	Peak arbutamine
Endocardial	0.90 ± 0.07	0.84 ± 0.07	0.55 ± 0.06*	1.00 ± 0.08	0.95 ± 0.09	1.85 ± 0.18†‡
Midmural	0.88 ± 0.07	0.85 ± 0.07	0.68 ± 0.08*	0.96 ± 0.09	0.93 ± 0.08	2.11 ± 0.21†‡
Epicardial	0.97 ± 0.10	0.96 ± 0.09	1.12 ± 0.15*	1.07 ± 0.12	1.01 ± 0.11	2.54 ± 0.31†‡
Transmural	0.92 ± 0.08	0.88 ± 0.08	0.78 ± 0.09	1.00 ± 0.09	0.96 ± 0.09	2.22 ± 0.23‡

*$P < 0.05$ vs. stenosis.
†$P < 0.001$ vs. stenosis.
‡$P < 0.001$ normal vs. stenosis zones.
Peak arbutamine: 250 ng/kg/min. Results (mL/min/g) are expressed as mean ± SEM.

increase systolic thickening at any dose of arbutamine (21.2% ± 2.4% to 16.4% ± 3.7%, $P < 0.05$). At the peak arbutamine dose of 250 ng/kg/min, thickening was greater in the normal zone (from 16.3% ± 1.8% to 23.0% ± 2.7%).

Regional Myocardial Blood Flow

In the stenotic zone, myocardial blood flow was unaffected by placement of the LAD critical stenosis; in the normal zone, the mean transmural flow of 0.96 ± 0.09 mL/min/g at baseline increased to 2.22 ± 0.23 mL/min/g at the time of peak arbutamine ($P < 0.001$; Table 3).

Arbutamine caused a significant increase in flow in all layers of the normal zone (endocardial, 95%; midmural, 127%; and epicardial, 152% [$P < 0.001$ vs. stenosis; Fig. 2]), whereas flow in the stenotic zone was reduced in the endocardial and midmural layers (35% and 20%, respectively) and increased 11% in the epicardial layer ($P < 0.001$). Arbutamine at 250 ng/kg/min increased transmural flow in the normal zone by a factor of 2 to 2.5 times resting flow. Transmural flow reserve was absent in the stenotic zone.

Stenotic-to-Normal Ratios for Myocardial Blood Flow, MIBI Activity, and ^{201}Tl Activity

Figure 3 compares activity on γ-well counting, activity on ex vivo imaging, and the mean stenotic-to-normal ratios for myocardial flow with radiolabeled microspheres at the time of peak arbutamine for MIBI and ^{201}Tl injections. The lower the ratio, the greater was the heterogeneity in flow or MIBI and ^{201}Tl activity between the stenotic and normal zones. A threshold of 0.75 for the stenotic-to-normal image count ratio is often used on quantitative perfusion imaging in clinical settings to distinguish abnormal stress-induced perfusion defects from the regional heterogeneity of tracer activity in healthy individuals (*16*). As shown in Figure 3, MIBI activity ratios markedly underestimated the flow disparity at the time of MIBI injection ($P < 0.001$). Despite a mean stenotic-to-normal flow ratio of 0.36 ± 0.03, with a 2:1 arbutamine-induced flow disparity between the normal and stenotic zones, the γ-well MIBI activity ratios and ex vivo image count ratios were 0.84 ± 0.05 and 0.77 ± 0.02 ($P < 0.001$), respectively. The defect count ratios for ^{201}Tl at the time of peak arbutamine stress were greater than those

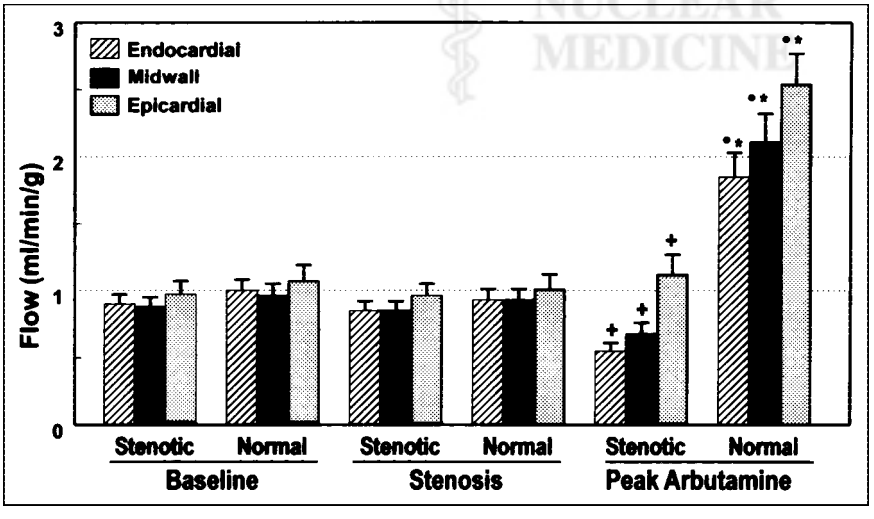

FIGURE 2. In stenotic zone, myocardial blood flow was unaffected by placement of critical stenosis. Arbutamine caused significant increase in flow in all layers of normal zone (endocardial = 95%; midmural = 127%, epicardial = 152%; *$P < 0.001$ vs. stenosis). During peak arbutamine, stenotic-zone flow decreased in endocardial (down 35%) and midmural (down 20%) layers and increased slightly (up 11%) in epicardial layer (†$P < 0.05$ vs. stenosis; •$P < 0.001$ normal vs. stenotic zone).

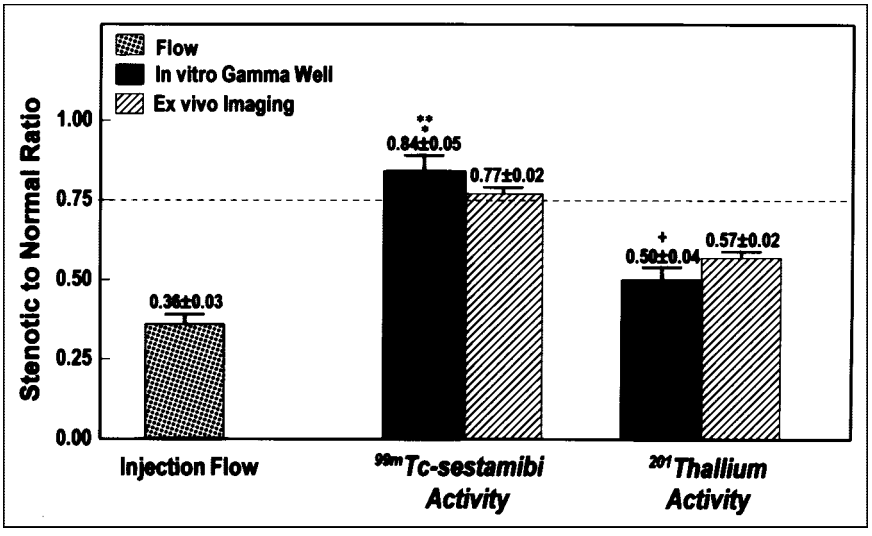

FIGURE 3. Mean stenotic-to-normal ratios for myocardial flow measured with radiolabeled microspheres and for ^{99m}Tc-MIBI and ^{201}Tl activity by in vitro γ-well counting and by ex vivo imaging (*$P <$ 0.001 vs. ^{201}Tl activity; **$P < 0.001$ vs. flow; †$P < 0.001$ vs. flow). ^{99m}Tc-MIBI activity ratios significantly underestimated arbutamine-induced flow disparity.

for MIBI, 0.50 ± 0.04 ($P < 0.001$) by γ-well counting and 0.57 ± 0.02 by ex vivo imaging. Figure 4 shows a representative example of anteroseptal perfusion defects for ^{201}Tl (0.49) and MIBI (0.79) on the gamma camera images of myocardial slices. Defects were of far greater magnitude on the ^{201}Tl images.

Comparison of Effect of Arbutamine Stress and Dobutamine Stress on MIBI Uptake

Figure 5 is a composite plot of mathematic curve fits relating normalized myocardial uptake of ^{201}Tl and MIBI versus regional myocardial blood flow during arbutamine stress. The raw data from which these curve fits were derived represent each of the 72 myocardial tissue samples taken from the 8 dogs and normalized to the activities at the resting flow rate of 1.0 mL/min/g. Shown for comparison are the curve fits for MIBI during adenosine or dobutamine stress from our previous studies (*2*,*16*). The curve fits are based on the solute transport model of Gosselin and Stibitz (*19*). As can be seen, during arbutamine stress, myocardial MIBI uptake begins to plateau as flow increases 1 to 1.5 times normal flow, and myocardial MIBI uptake is superimposable on the curve derived from the previous dobutamine–MIBI studies (*2*). With both inotropic stressors, the attenuation of MIBI uptake was greater than previously observed with adenosine and MIBI (*16*). The relationship between uptake of ^{201}Tl and flow during arbutamine stress is more favorable than that between MIBI and flow.

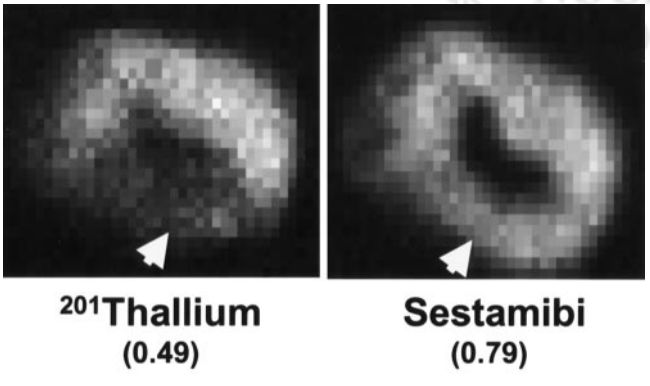

FIGURE 4. Ex vivo images from representative dog. Arrows indicate location of ^{201}Tl and ^{99m}Tc-MIBI perfusion defects. Numbers in parentheses below each image are stenotic-to-normal defect count ratios.

DISCUSSION

In this canine model of critical coronary stenoses with no flow reserve, intravenous infusion of arbutamine was followed by administration of ^{201}Tl and MIBI. We found that both tracers significantly underestimated the arbutamine-induced flow heterogeneity between normal and stenotic regions, with the underestimation being greater for MIBI. Myocardial MIBI uptake underestimated the arbutamine-induced hyperemia in normal myocardium to the same extent as we had previously reported for dobutamine stress (*2*). This finding suggests that arbutamine also adversely affects myocardial MIBI binding, presumably by enhancing calcium entry into the mitochondria, with subsequent reduction of the mitochondrial membrane potential. MIBI uptake with arbutamine stress underestimates the physiologic severity of coronary stenoses. This underestimation of stenosis severity was previously observed in clinical studies by Ogilby et al. (*11*).

We observed a flat systolic thickening in response to arbutamine in myocardium with no flow reserve. Systolic thickening failed to increase during arbutamine infusion when flow reserve in the LAD bed was absent. This response was similar to what was observed with dobutamine in the same canine model (*2*).

Myocardial perfusion imaging is based on the principle that flow heterogeneity in coronary vascular beds can be detected as a perfusion defect (*6*). In our study, arbutamine increased blood flow in normal myocardium by a factor of approximately 2.5 times baseline flow. Although this in-

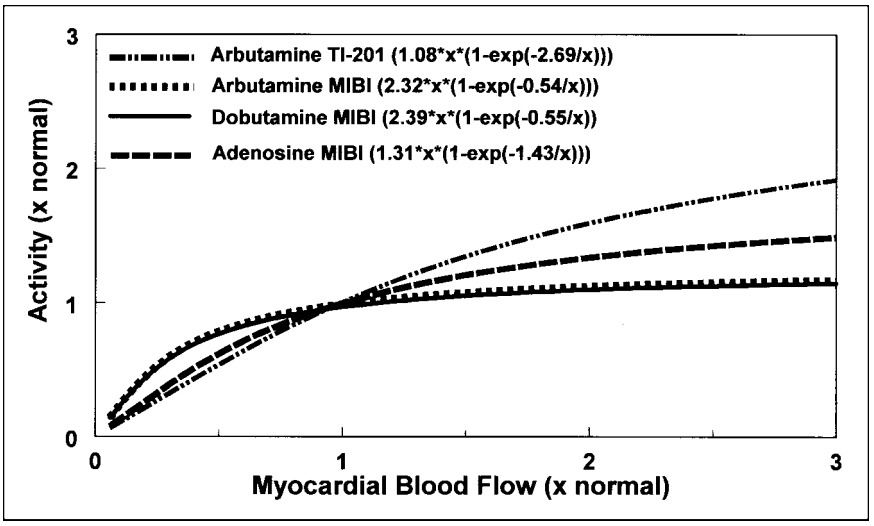

FIGURE 5. Mathematic curve fits relate normalized ^{99m}Tc-MIBI and ^{201}Tl activities as function of arbutamine flow. Shown for comparison are adenosine and dobutamine MIBI uptake curves from our previous studies. Note that MIBI uptake with either dobutamine or arbutamine was comparable. Both inotropic stressors produced greater reduction in MIBI uptake than was observed with adenosine.

crease in blood flow was smaller than the 4-fold increase seen with vasodilator stress agents (*2–6,16*), both the relative increase from baseline and the peak flow achieved were comparable with those reported previously for dobutamine stress (*2,6,7*).

Between myocardial regions supplied by normal arteries and myocardial regions supplied by stenotic arteries, arbutamine stress produces a flow disparity (2.5 times in this study) that is adequate for perfusion imaging in combination with a radionuclide tracer, which is distributed in the myocardium in proportion to flow over this range. Also like dobutamine, arbutamine produces secondary vasodilatation because of an increase in myocardial oxygen demand (*6–12*).

Myocardial uptake of MIBI and ^{201}Tl depend on myocardial blood flow and myocardial extraction of the tracer. Myocardial uptake of MIBI, a lipophilic cationic molecule, is thought to occur through electric charge–driven diffusion across sarcolemmal membranes, with cellular retention in mitochondrial membranes being caused by the negative transmembrane potential (*18–21*). In this study, the arbutamine stress response produced a relationship between myocardial blood flow and MIBI uptake comparable with that seen for dobutamine stress in the same canine models (*2*).

The quantitative MIBI perfusion defects produced by arbutamine stress in this study were relatively mild and would have been difficult to distinguish from the regional heterogeneity in tracer activity observed in healthy individuals. The myocardial uptake of ^{201}Tl is more closely proportional to flow during arbutamine stress; hence, ^{201}Tl may be a better imaging agent.

A limitation of this study is that the effects of arbutamine stress may have been influenced by the use of a pentobarbital-anesthetized canine model. However, the response of myocardial blood flow to arbutamine was similar to that observed in our previous studies of dobutamine stress in a similar experimental model and were comparable with the response reported for conscious humans (*2,9,16*). We confirmed absence of flow reserve in the stenotic zone by microsphere-derived tissue blood flow measurements, using a highly accurate in vitro γ-well counting technique. The responses to arbutamine stress in patients with chronic coronary artery disease may differ from the responses observed in this canine model of experimentally created coronary artery stenoses.

CONCLUSION

This experimental study showed that in the presence of coronary stenoses that abolished regional flow reserve, myocardial MIBI uptake, in comparison with ^{201}Tl uptake, significantly underestimated the arbutamine-induced flow heterogeneity. The attenuation of MIBI uptake and diminished defect contrast during arbutamine stress were comparable with those previously reported for dobutamine stress. Mild stenoses may be missed using either dobutamine or arbutamine. Such defects may be better detected using ^{201}Tl.

ACKNOWLEDGMENTS

The authors appreciate the assistance of Jerry Curtis with manuscript preparation. This study was supported by a grant from Gensia Automedics, Inc. (San Diego, CA), and by a research grant from Bristol Myers Squibb Medical Imaging (North Billerica, MA).

REFERENCES

1. Bach D, Cohen JL, Fioretti PM, et al. Safety and efficacy of closed-loop arbutamine stress echocardiography for detection of coronary artery disease. *Am J Cardiol.* 1998;81:32–35.
2. Calnon DA, Glover DK, Beller GA, et al. Effects of dobutamine stress on myocardial blood flow, ^{99m}Tc sestamibi uptake, and systolic wall thickening in the presence of coronary artery stenoses. *Circulation.* 1997;96:2353–2360.
3. Hartley C, Latson L, Michael L, Seidel C, Lewis R, Entman M. Doppler measurement of myocardial thickening with a single epicardial transducer. *Am J Physiol.* 1983;245:H1066–H1072.
4. Heymann MA, Payne BD, Hoffman JIE, Rudolph AM. Blood flow measurements with radionuclide-labeled particles. *Prog Cardiovasc Dis.* 1977;20:55–79.
5. Calnon DA, Ruiz M, Vanzetto G, Watson DD, Beller GA, Glover DK. Myocar-

dial uptake of Tc-99m sestamibi during dobutamine stress is enhanced by ruthenium red, an inhibitor of mitochondrial calcium influx [abstract]. *Circulation.* 1997;96(suppl):I-687.
6. Iskandrian AS, Verani MS, Heo J. Pharmacologic stress testing: mechanism of action, hemodynamic responses, and results in detection of coronary artery disease. *J Nucl Cardiol.* 1994;1:94–111.
7. Segar DS, Ryan T, Sawada SG, Johnson M, Feigenbaum H. Pharmacologically induced myocardial ischemia: a comparison of dobutamine and dipyridamole. *J Am Soc Echocardiogr.* 1995;8:9–14.
8. Shehata AR, Ahlberg MA, Gilliam LD, et al. Direct comparison of arbutamine and dobutamine stress testing with myocardial perfusion imaging and echocardiography in patients with coronary disease. *Am J Cardiol.* 1997;80:716–720.
9. Severi S, Underwood R, Mohiaddin RH, Boyd H, Paterni M, Camici PG. Dobutamine stress: effects on regional myocardial blood flow and wall motion. *J Am Coll Cardiol.* 1995;26:1187–1195.
10. Young M, Pan W, Bullough D, et al. Characterization of arbutamine stress agent for diagnosis of coronary artery disease. *Drug Dev Res.* 1994;32:19–28.
11. Ogilby D, Molk B, Iskandrian S. Hemodynamic effects of arbutamine. *Am J Cardiol.* 1998;82:699–702.
12. Bach DS, Armstrong WF. Adequacy of low-stress arbutamine to provoke myocardial ischemia during echocardiography. *Am J Cardiol.* 1995;76:259–262.
13. Hendel R, Kostuk W, Beanlands R, et al. Comparison of Tc-99m sestamibi perfusion imaging and echocardiography using an arbutamine infusion for the detection of coronary artery disease. *Am J Cardiol.* 1997;79:1518–1521.
14. Kiat H, Iskandrian A, Villegas B, Starling M, Berman D. Arbutamine stress thallium-201 single photon emission computed tomography using a computerized closed-loop delivery system. *J Am Coll Cardiol.* 1995;26:1159–1167.
15. Yun JJ, Wu JC, Heller EN, et al. Dobutamine stress has limited value for enhancing flow heterogeneity in the presence of a moderate stenosis when used in conjunction with Tc-99m sestamibi imaging [abstract]. *J Am Coll Cardiol.* 1995;25(suppl A):217A.
16. Glover DK, Ruiz M, Edwards NC, et al. Comparison between ^{201}Tl and ^{99m}Tc sestamibi uptake during adenosine-induced vasodilation as a function of coronary stenosis severity. *Circulation.* 1995;91:813–820.
17. Crane P, Laliberte R, Heminway S, Thoolen M, Orlandi C. Effect of mitochondrial viability and metabolism on technetium-99m–sestamibi myocardial retention. *Eur J Nucl Med.* 1993;20:20–25.
18. Kettler T, Krahwinkel W, Wolfertz J, et al. Arbutamine stress echocardiography. *Eur Heart J.* 1997;18(suppl D):D24–D30.
19. Gosselin RE, Stibitz GR. Rates of solute absorption from tissue depots: theoretical considerations. *Pflugers Arch.* 1970;318:85–98.
20. Piwnica-Worms D, Kronauge JF, Chiu ML. Uptake and retention of hexakis (2-methoxy- isobutyl isonitrile) technetium (I) in cultured chick myocardial cells: mitochondrial and plasma membrane potential dependence. *Circulation.* 1990; 82:1826–1838.
21. Hammond HK, McKirnan MD. Effects of dobutamine and arbutamine on regional myocardial function in a porcine model of myocardial ischemia. *J Am Coll Cardiol.* 1994;23:475–842.